ЭЛЕКТРОФИЗИКА, ЭЛЕКТРОФИЗИЧЕСКИЕ УСТАНОВКИ/ELECTROPHYSICS, ELECTROPHYSICAL INSTALLATIONS

DOI: https://doi.org/10.60797/IRJ.2025.160s.23

NUMERICAL INVESTIGATION OF PARALLEL-PLATE MAGNETIC COMPRESSION LINE

Research article

Patrakov V.E.[1,*]
[1] ORCID : 0000-0002-2874-6379;
[1] Institute of Electrophysics UB RAS, Ekaterinburg, Russian Federation

* Corresponding author (vitpatrakov[at]gmail.com)

Abstract

Magnetic compression lines are novel picosecond pulsed power devices, which open the possibility of generating picosecond electrical pulses with peak power of over 100 GW. Recently, it has been found that pulse duration in magnetic compression lines is greatly influenced by the dispersion of dominant quasi-TEM propagation mode of dual-dielectric coaxial structure. This work numerically investigates the operation of a magnetic compression line based on dual-dielectric parallel-plate transmission line, which also exhibits quasi-TEM-type dispersion. Based on full-wave simulation, typical modes of pulse compression are determined, and the influence of input pulse parameters and line geometry on pulse compression is evaluated. The analysis shows that the presence of quasi-TEM-type dispersion affects the process of pulse compression in the same way regardless of the type of transmission line used.

Keywords: pulsed power, picosecond pulse, transmission line, ferrite.

ЧИСЛЕННОЕ ИССЛЕДОВАНИЕ ПОЛОСКОВОЙ ЛИНИИ МАГНИТНОЙ КОМПРЕССИИ

Научная статья

Патраков В.Е.[1,*]
[1] ORCID : 0000-0002-2874-6379;
[1] Институт электрофизики УрО РАН, Екатеринбург, Российская Федерация

* Корреспондирующий автор (vitpatrakov[at]gmail.com)

Аннотация

Линии магнитной компрессии являются современными устройствами мощной импульсной техники пикосекундного диапазона, позволяющими генерировать пикосекундные электрические импульсы с пиковой мощностью более 100 ГВт. Недавно было обнаружено, что на длительность импульса в линиях магнитной компрессии значительное влияние оказывает дисперсия основной волны квази-ТЕМ в коаксиальной структуре с двумя диэлектрическими слоями. В данной работе проведено численное исследование линии магнитной компрессии на основе линии передачи симметрично-полоскового типа с двумя диэлектрическими слоями, в которой также присутствует дисперсия типа квази-ТЕМ. На основании полноволнового моделирования установлены типичные режимы компрессии импульса, а также выявлено влияние параметров входного импульса и геометрии линии на компрессию импульса. Анализ показал, что присутствие дисперсии типа квази-ТЕМ одинаково влияет на процесс компрессии импульса независимо от используемого типа линии передачи.

Ключевые слова: мощная импульсная техника, пикосекундный импульс, линия передачи, феррит.

Introduction

Picosecond high-power electrical pulses are in demand in experimental physics for studying delayed breakdown processes in various media [1], generating high-power pulses of X-ray and microwave radiation [2], [3], generating and studying high-energy runaway electron beams in atmospheric air [4], [5], [6], and calibrating fast radiation detectors and voltage sensors by measuring their impulse response [7], [8]. Magnetic compression lines (MCL) are novel pulsed power devices that are able to produce such pulses. Pioneering works on MCLs were conducted in 2017–2019 [9], [10], [11], [12], followed by the construction of MCL-based generators with record pulse parameters described in [13], [14]. The design of an MCL, shown in Fig. 1, consists of a coaxial transmission line with ferrite rings set on the inner conductor, while the rest of the line volume is filled with transformer oil (not shown in the picture) for the purposes of insulation. The ferrite is magnetized to the state of saturation by an external solenoid. When a high-voltage input pulse is supplied to one end of the line, it propagates along it in travelling wave mode. At certain parameters of the input pulse, its energy is redistributed during the propagation in such a way that pulse amplitude increases and pulse duration decreases (Fig. 2). Usually during compression, the duration of the pulse is reduced by a factor of 3–4, and its amplitude is increased by a factor of 2. By cascading the lines, an exponential increase in amplitude and decrease in pulse duration are achieved. The development of MCL-based pulsed power systems at the Institute of Electrophysics UB RAS has allowed building a fully-solid state (without the use of commutating spark gaps) picosecond pulse generator with record pulse parameters: peak power of 100 GW at pulse duration of about 100 ps (FWHM) [14]. The generator consists of a solid-state high-voltage driver S-500 [15] based on SOS-diodes, and four cascaded MCL-based pulse compression stages. Peak voltage produced by the generator in a 48-Ω transmission line is about 2.2 MV.

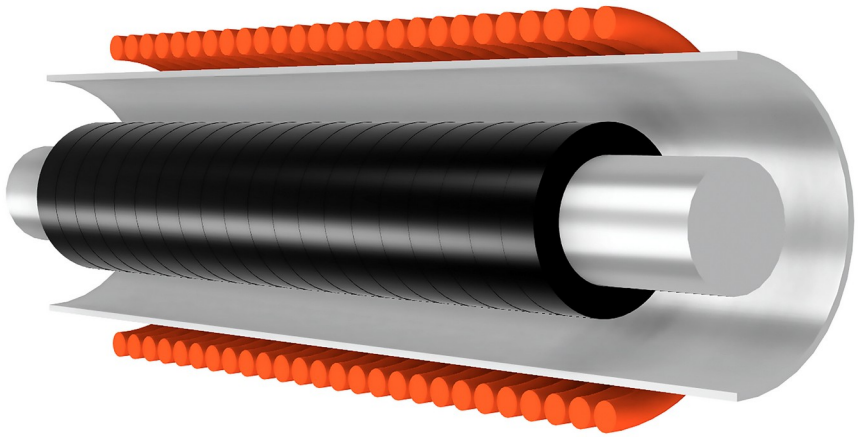

Figure 1 - Sectional view of a coaxial magnetic compression line
DOI: https://doi.org/10.60797/IRJ.2025.160s.23.1

Note: transformer oil filling the line is not shown

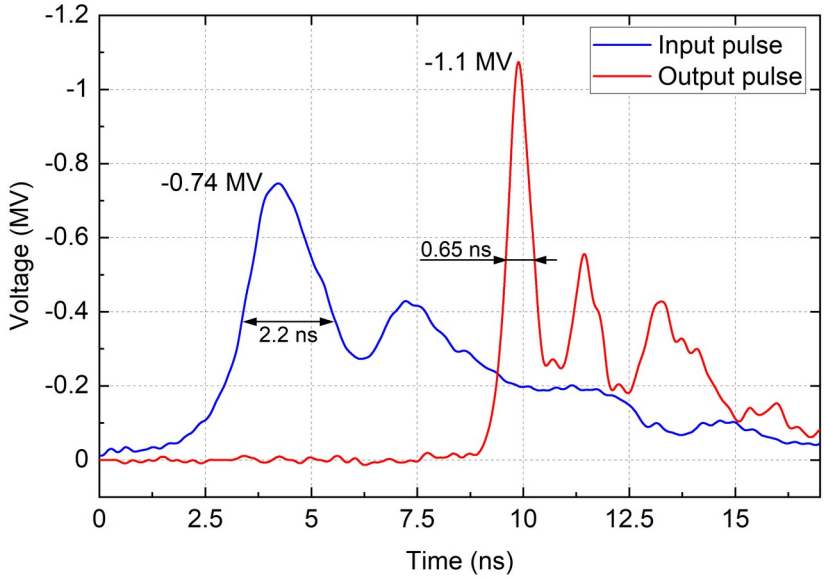

Figure 2 - Typical experimental waveforms of pulse compression in MCL obtained during experiments described in [11]
DOI: https://doi.org/10.60797/IRJ.2025.160s.23.2

Note: the pulses are plotted without synchronization

The physical processes underlying the operation of magnetic compression lines are currently under study. First attempts at describing the pulse compression process were based on existing theory for gyromagnetic nonlinear transmission lines, which are high-power microwave devices of similar design [16], [17]. This theory was based on the induction of oscillating voltage in the line cross-section by the quasi-periodic precessional motion of magnetization vector in ferrite. However, this theory fails in predicting pulse duration shaped by MCLs, frequently underestimating it by an order of magnitude [14]. With the development of full-wave MCL simulation based on numerical solution of Maxwell's equations, it was found that an important factor affecting MCL operation is its radial inhomogeneity — the presence of two radial dielectric layers, transformer oil and saturated ferrite [14], [18], [19]. It was found that such a design, traditionally used solely to increase the dielectric strength of the line (the oil has much higher breakdown voltage than ferrite), has a great effect on the parameters of output pulse of the MCL compared to a hypothetical line fully-filled with ferrite. In this design, the duration of the output pulse becomes directly related to the roundtrip time of the electromagnetic wave between the line conductors due to the dispersion of the formed quasi-TEM (TM_{00}) propagating mode. The dispersion of this mode is of dielectric-waveguide type and manifests itself as the

increased group delay of high-frequency signal components compared to low-frequency ones due to former concentrating inside the saturated ferrite layer, consecutively undergoing reflection from the inner conductor and total internal reflection from the boundary between the ferrite and the oil.

Based on the data from microwave engineering literature [20], [21] one can conclude that the described quasi-TEM dispersive behavior is characteristic for a number of transmission lines with two dielectric layers (one of which can be air): Goubau line, microstrip line, metal-backed dielectric waveguides, etc. This poses the question of there being a similar pulse-duration-limiting effect in MCLs based on types of transmission lines other than coaxial. The simplest example of a line with the quasi-TEM type of dispersion is a parallel-plate transmission line with two dielectric layers. Such a structure, if it were to replicate the main features of the usual MCL operation, could serve as a simplified planar model of a usual MCL which potentially could be described by a system of equations with closed-form solutions, acting as a basis for the analytical theory of MCL operation. In view of this, in the present work a full-wave model of an MCL based on a parallel-plate line was created, and numerical experiments concerning the line operation were performed. The main goals of numerical experiments were to investigate the operation of a planar transmission line structure with a ferrite slab as a pulse compressor, and to test the replication of the influence of line cross-sectional geometry on output pulse parameters seen in conventional coaxial MCLs.

Model description

The model, as the author's previously developed model for a coaxial MCL [22], [23], was based on the coupled system of Maxwell's equations written using magnetic vector potential **A** and the Landau-Lifshitz-Gilbert (LLG) equation. The latter describes the motion of magnetization vector **M** in saturated ferrite. It should be noted that due to the nonlinear nature of a ferrite transmission line, the principle of superposition of the fields does not hold true, hence, commonly used Fourier analysis is not applicable and only time-domain analysis is possible. The time-dependent model equations were taken as follows:

$$\frac{1}{\mu_0}\nabla \times (\nabla \times \mathbf{A} - \mu_0 \mathbf{M}) + \sigma \frac{\partial \mathbf{A}}{\partial t} + \varepsilon_0 \varepsilon \frac{\partial^2 \mathbf{A}}{\partial t^2} = 0 \quad (1)$$

$$\frac{d\mathbf{M}}{dt} = -\gamma \mu_0 \left[\mathbf{M} \times \left(\frac{1}{\mu_0}\nabla \times \mathbf{A} - \mathbf{M}\right)\right] + \frac{\alpha}{M_s}\left[\mathbf{M} \times \frac{d\mathbf{M}}{dt}\right] \quad (2)$$

Here, **A** is the magnetic vector potential, and **M** is the magnetization vector. The constants ε_0 and μ_0 are permittivity and permeability of vacuum, and γ is the absolute value of spin gyromagnetic ratio of an electron, equal to $1.76 \cdot 10^{11}$ rad/(s·T). Material properties are defined through electrical conductivity σ, relative dielectric constant ε, and the properties which are specific to ferrite medium: precession damping coefficient α and magnitude of saturation magnetization M_s. In equation (2) the first term on the righthand side is modified from the usual LLG form to include the coupling to the equation (1).

The system (1)-(2) needs to be expanded into the coordinate form for numerical solution, which is different for Cartesian and curvilinear coordinates due to the presence of the curl operator. Previously, for coaxial MCLs this was done in cylindrical coordinates. In this work the system was expanded for 2D planar geometry, taking the x, y, and z components of the vectors and setting the spatial derivatives in the curl operator with respect to the out-of-plane axis equal to zero.

The geometry of the system is schematically presented in Fig. 3. Fig. 3a shows a 3D sectional view of the parallel-plate ferrite-slab-loaded transmission line, and the magnetizing solenoid. Fig. 3b shows the actual simulation geometry representing the longitudinal cross-section of the structure. It is important to note that in such simulation an infinite extent of the line in the out-of-plane direction is assumed, which can be thought of as a good approximation for the geometry in Fig. 3a when the width of the line is much greater than the distance between the conductors. For a baseline geometry, conductor distance of 16 mm and ferrite filling factor k_f of 0.375 was chosen (6 mm thickness of ferrite slab). The parameters of the ferrite were set based on the known values for nickel-zinc ferrite of M200VNP type [14]: relative permittivity of 12, saturation magnetization of 300 kA/m, and damping coefficient α of 0.1. Transformer oil with a relative permittivity of 2.25 was taken as the insulating medium in the line. The external geometry consists of the solenoid and surrounding air (Fig. 3b) and is used in preliminary magnetostatic calculations only.

Boundary conditions include the perfect electric conductor boundaries representing the conductors of the line, and scattering boundary conditions at the start and the end of the line, which act as matched terminations and absorb any reflected waves. One of the scattering boundary conditions acts as an excitation, exciting a uniform electric field corresponding to the TEM mode in the parallel-plate line. The waveform and amplitude of the field are set by the parameters of the input voltage pulse. To match the TEM excitation and termination to the inhomogeneous ferrite part of the line, homogeneous oil-filled sections of 40 mm in length are added on both ends of the ferrite-filled section.

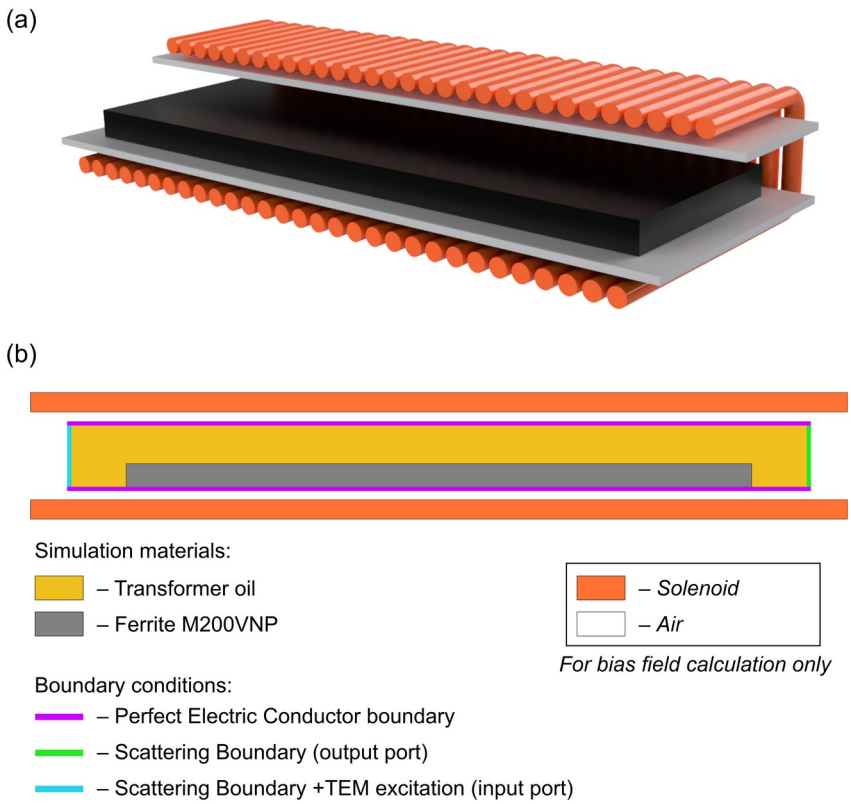

Figure 3 - Sectional view of a parallel-plate magnetic compression line partially filled with ferrite *(a)*; 2D simulation geometry – longitudinal section of the line *(b)*

DOI: https://doi.org/10.60797/IRJ.2025.160s.23.3

The described model was solved numerically using the finite-element method software COMSOL Multiphysics. A preliminary step calculates the static distribution of the magnetizing field from an external solenoid. During the main study step, the system (1)-(2) is solved. The equation (1) is solved in the whole geometry, while equation (2) is solved only in the part of the geometry containing ferrite. The boundary Brown equation [24], which serves as the boundary condition in problems with magnetization in a limited body, is fulfilled here naturally due to the weak-form implementation of the finite-element method. For the discretization, a triangular mesh with quadratic vector elements was chosen. Time stepping is performed using the generalized-alpha algorithm, and the time step and mesh size are chosen using the method described in [23].

Influence of input pulse duration on pulse shaping mode

The first set of numerical experiments consisted of varying the duration of the input pulse in the baseline geometry and observing its influence on the output waveform of the line. In nonlinear dispersive wave systems, the shape, duration, and amplitude of the input wave affect the waveform transformation [25]. In an MCL the nonlinearity comes from the field-dependent permeability of saturated ferrite, and the dispersion comes either from the waveguiding effect due to the formation of the quasi-TEM-type mode, or due to the gyromagnetic properties of the line, depending on magnetic field strength in the line [18].

The shape of the input pulse in calculations was set as a Gaussian function. Following the experimental convention, the pulses of negative polarity were used. The value of bias magnetic field was set to 100 kA/m. It was found that for different input pulse amplitudes the general modes of pulse shaping remain the same. Typical waveforms of these modes are presented in Fig. 4 for input pulse amplitude of 1400 kV. Depending on the input pulse duration, the output pulse consists of one or several nonlinear oscillation peaks, which can be recognized as solitary waves or solitons [14]. Under short pulse duration (Fig. 4a), 280 ps for the studied conditions, the amplitude of the pulse practically does not change, and its shape transforms to the one having steeper top and more gradual lower parts of the pulse. This shape matches the function $\mathrm{sech}^2(t)$, shown in Fig. 4a by a dashed line, which is characteristic for solitons formed in Korteweg-De-Vries-like systems [25].

If on the contrary, pulse duration is quite long, for example 1400 ps for the studied conditions, the line operates in the nonlinear microwave regime, generating several peaks of soliton-like oscillations (Fig. 4b). In this regime peak power increase can achieve 2.6 times, however, the formation of additional unwanted peaks of relatively high amplitude prohibits the use of this regime for pulse compression.

It is evident that in the context of pulse compression the operating mode of the line is set by the duration of the input pulse at a given amplitude. One must choose the input pulse duration as an optimum between the amount of unwanted post-pulse signal and the desired peak power increase, since these quantities are inversely related. Usually, in MCL experiments the power increase of 2 is chosen. Such a mode is presented in Fig 4c, with an input pulse duration of 560 ps. In these conditions peak power is increased twofold at the cost of the formation of the second peak. However, the amplitude of the second peak is

relatively low, 1/3 of the amplitude of the main peak. This operation mode is similar to the usual mode implemented in multi-gigawatt coaxial MCLs. Comparison with $sech^2(t)$ function presented in Fig. 4c shows good agreement of the main peak with the expected soliton waveform.

Overall, the conducted set of numerical experiments leads us to the following conclusions. The parallel-plate ferrite line exhibits the pulse shaping modes analogous to those observed in coaxial ferrite lines. It nonlinearly transforms a high-voltage bell-shaped pulse into a pulse consisting of one or several solitons with a shape close to $sech^2(t)$ curve, depending on input pulse duration at a given amplitude. Analogously to other soliton systems, for bell-shaped input pulses the number of generated soliton peaks can approximately be found as the integer part of the relation of input pulse duration t_{in} to a characteristic time τ, equal to the soliton duration (FWHM) at an amplitude equal to that of the input pulse [26], [27].

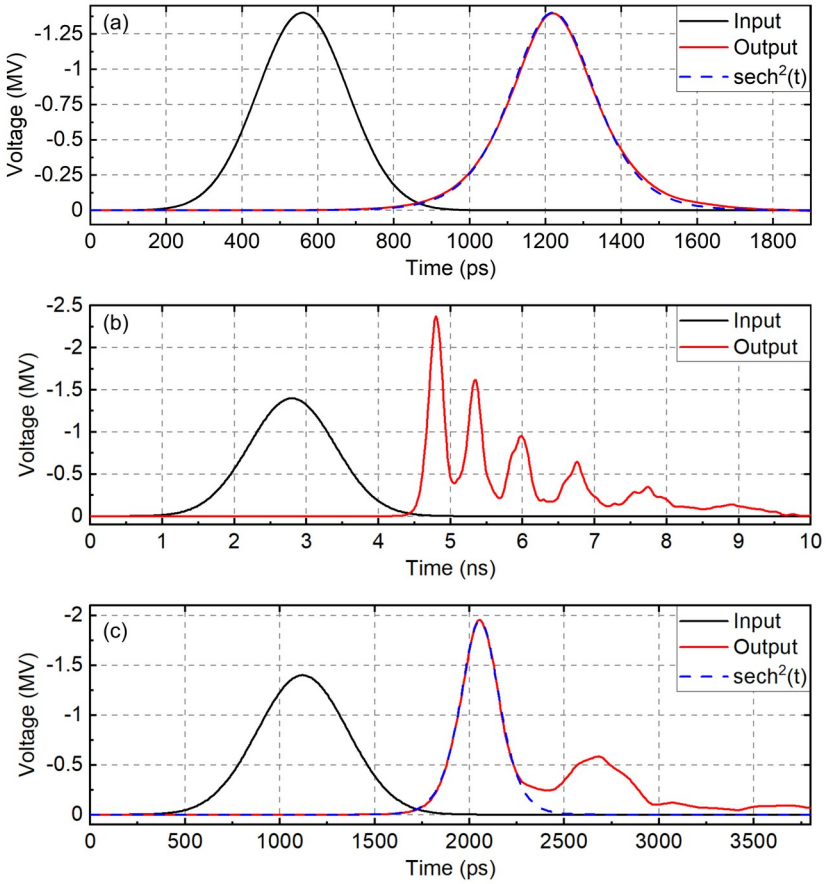

Figure 4 - Typical modes of pulse shaping:
(a) single-soliton shaping, *(b)* multi-soliton decomposition (nonlinear oscillations generation), *(c)* optimal pulse compression
DOI: https://doi.org/10.60797/IRJ.2025.160s.23.4

Note: the input and output pulses are plotted without synchronization

From the waveforms presented in Fig. 4a it was found that at the given input pulse amplitude the duration of a single soliton and, hence, the value of τ is equal to 260 ps. In the case presented in Fig. 4a, the relation $t_{in}/\tau \approx 1.1$, and no additional solitons are formed; the input Gaussian pulse is only reshaped to match the $sech^2(t)$ soliton waveform. In Fig. 4b, $t_{in}/\tau \approx 5.4$, hence 5 soliton peaks are formed, and the leftover energy forms a dispersive sixth peak [25] due to an excessive value of t_{in}. Finally, in Fig. 4c, $t_{in}/\tau \approx 2.2$, and correspondingly, two soliton peaks are formed.

Typical dynamics of pulse compression obtained in the simulations for the optimal compression mode is presented in Fig. 5. The transformation of the pulse consists of initial pulse sharpening in a shock-wave manner (0 – 40 mm), subsequent appearance of oscillations on top of the pulse due to dispersive decay of sharpened pulse front (40 – 80 mm), and the decomposition of the pulse into two solitons, during which the first one obtains higher amplitude and velocity than the second one (80 – 360 mm). This dynamics is analogous to the one seen in coaxial MCLs [14] and is characteristic for Korteweg-de-Vries-like soliton systems.

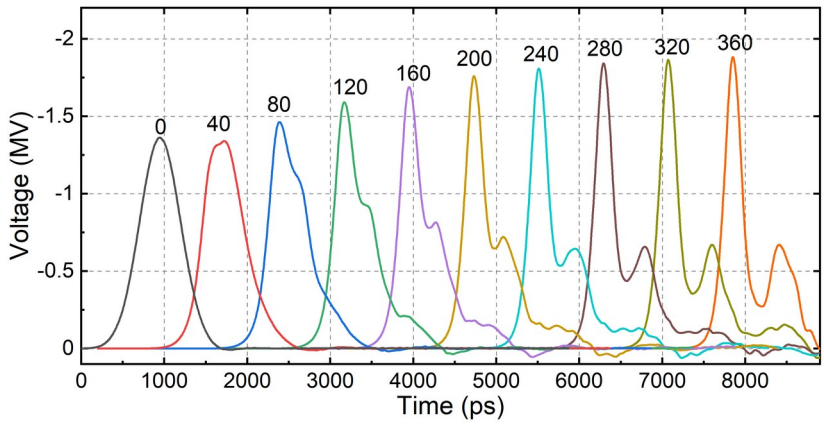

Figure 5 - Dynamics of pulse compression on optimal mode
DOI: https://doi.org/10.60797/IRJ.2025.160s.23.5

Note: the number above each pulse corresponds to the distance from the start of the ferrite section in mm; the pulses are plotted without synchronization

It is apparent that to obtain a desired pulse shaping mode in a given line, one needs to know its value of τ. In general, τ will depend on line cross-sectional geometry due to the waveguide nature of its dispersion, and the value of biasing magnetic field and input pulse amplitude due to nonlinear ferrite properties. Experimental observations on coaxial MCLs show that for similar pulse parameters, conductor distances and ferrite filling factors of the line, the value of τ is roughly independent of pulse amplitude and is close to the calculated time of electromagnetic wave propagation between line conductors T_0 multiplied by 2 [14]. For the studied geometry, the value of $2T_0$ is approximately 270 ps, which is indeed close to 260 ps found from described numerical calculations.

Influence of pulse amplitude and ferrite filling factor on optimum compression mode parameters

As was stated above, there exists an optimum pulse compression mode, in which peak power of the pulse is increased by a factor of 2. To obtain such a mode, one must supply an input pulse with specific amplitude $V_{in,\,opt}$ and duration (FWHM) $t_{in,\,opt}$ for a line of a given cross-sectional geometry. The set of numerical experiments described in this subsection is conducted for evaluating the dependencies between $V_{in,\,opt}$, $t_{in,\,opt}$ and compression parameters for different values of ferrite filling factor k_f, defined as the ratio of ferrite slab thickness to the distance between line conductors.

The results of numerical experiments are presented in Fig. 6. Fig. 6a shows the dependence of $t_{in,\,opt}$ on $V_{in,\,opt}$. For low pulse amplitudes (300-400 kV), the optimal pulse duration is practically independent of k_f and decreases with increase in input pulse amplitude. With further increase in pulse amplitude, the curves for different values of k_f diverge and for pulse amplitudes of more than ~1000 kV the optimal pulse duration is practically independent of pulse amplitude, and decreases with decrease in k_f.

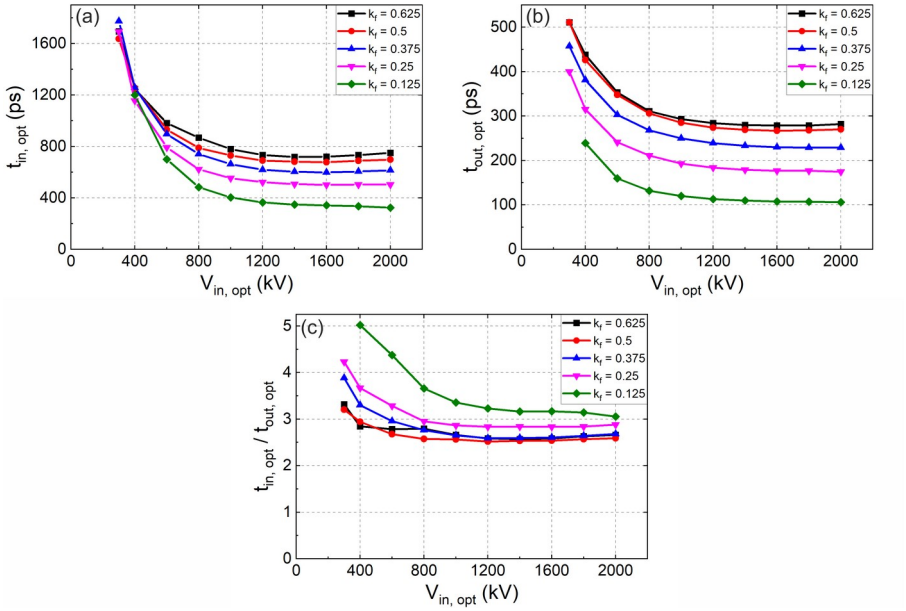

Figure 6 - Variation of optimal compression mode parameters with input pulse amplitude $V_{in, opt}$ and ferrite filling factor k_f : *(a)* optimal input pulse duration $t_{in, opt}$; *(b)* output pulse duration $t_{out, opt}$; *(c)* compression coefficient
DOI: https://doi.org/10.60797/IRJ.2025.160s.23.6

The observed dependence can be explained in terms of dispersion characteristics of dominant quasi-TEM mode (TM_0 mode in the case of a parallel-plate line) with a gyromagnetic filling [18]. The optimum pulse duration can be found from a characteristic time τ as $t_{in, opt} \approx 2\ \tau$, and τ directly depends on the shape of the dispersion curve of the line. In a line with composite ferrite-dielectric filling, the dispersion curve changes with a change in magnetic field of the pulse, as described in [18]. At low pulse amplitudes the frequency of gyromagnetic precession, determined by the magnetic field in the line, is lower than the inflection frequency of the quasi-TEM dispersion curve. Accordingly, the value of τ is determined by the average value of magnetic field in the cross-section of the line, which in this case depends only on pulse amplitude and not on the ferrite filling factor k_f. Thus, $t_{in, opt}$ also depends only on pulse amplitude.

With the increase in pulse amplitude, the magnetic field and the frequency of gyromagnetic precession increase, and $t_{in, opt}$ decreases, as can be seen in Fig. 5a for voltages of 300–400 kV. When the frequency of gyromagnetic precession approaches the k_f-dependent inflection frequency of quasi-TEM dispersion curve, the latter starts influencing the value of $t_{in, opt}$ as well (~500 kV). At high pulse amplitudes and corresponding magnetic fields (>1000 kV in Fig. 5a) the frequency of gyromagnetic precession becomes much higher than the inflection frequency of quasi-TEM dispersion curve**,** and only the latter influences the value of τ and $t_{in, opt}$. Due to this, optimal pulse duration becomes independent of pulse amplitude and is determined by the dispersion characteristics of the quasi-TEM mode.

The value of τ is inversely related to the inflection frequency of the quasi-TEM dispersion curve, and hence is proportional to its period. Due to the transverse-reflection mechanism of the propagation of dispersive guided waves, this period is proportional to the roundtrip time of electromagnetic wave between line conductors denoted as T_0, which for a line with saturated ferrite depends on the permittivities of ferrite ε_f (equal to 12) and transformer oil ε_{oil} (equal to 2.25):

$$T_0 = \frac{D \cdot \left(k_f \sqrt{\varepsilon_f} + (1 - k_f) \sqrt{\varepsilon_{oil}}\right)}{c} = \frac{D \cdot \left(k_f \left(\sqrt{\varepsilon_f} - \sqrt{\varepsilon_{oil}}\right) + \sqrt{\varepsilon_{oil}}\right)}{c} \quad (3)$$

Here D is distance between line conductors and c is speed of light in vacuum. As can be seen from (3), T_0 has a linear dependence on k_f. Due to that, τ and $t_{in, opt}$ are proportional to k_f as well, which explains the increase of the plateau level of the curves in Fig. 5a with increasing k_f.

Fig. 5b shows obtained dependencies of output pulse duration $t_{out, opt}$ on $V_{in, opt}$ for different values of k_f. It is seen that output pulse duration exhibits similar behavior to $t_{in, opt}$, showing the k_f-dependent plateau at input voltages with amplitude greater than ~1 MV. The reason for this can be assumed to be the proportionality between output pulse duration and τ , and the dependence of τ on line parameters described above. However, unlike in Fig. 5a, the curves in Fig. 5b do not converge at low values of input pulse amplitude. To analyze the correlation of data from Fig. 5a and Fig. 5b, the compression coefficient defined as the relation of input pulse duration to output pulse duration is plotted in Fig. 5c. Here one can observe that in all cases except k_f = 0.125 the curves exhibit the plateau at voltages higher than 1 MV, with the value of compression coefficient being in the range of 2.5-3. At lower input voltages, the compression coefficient increases. In the described framework of dispersion-defined operation modes, it can be stated that at voltages greater than 1 MV the presession frequency becomes so much greater than inflection frequency of quasi-TEM dispersion curve, that the temporal characteristics of line operation become field-independent and depend only on geometrical parameters.

The compression coefficient curve at k_f = 0.125 is noticeably different from the curves at other k_f values. Moreover, it was found that at k_f values greater than 0.625, the generated signal obtains additional modes of oscillation, which disrupt the compression process, hence such k_f values are absent from the above analysis. At the moment, the author cannot present a clear

explanation of these effects. In this work these problems were not studied further, and can only be stated as the evidence to the complexity of phenomena occurring in ferrite-filled nonlinear transmission lines.

However, from a practical point of view, the regimes with low and high values of k_f are of low importance, because due to design limitations and the need for high dielectric strength only the values of k_f close to 0.4-0.5 would be realized in practice. In view of that, for practical purposes, the most important effect described here is the existence of two regimes of optimal compression based on input pulse amplitudes. For pulse amplitudes lower than some threshold value (1 MV in this case) the first regime of optimal compression is realized, in which the durations of input and output pulse are influenced by input pulse amplitude due to gyromagnetic processes. For pulse amplitudes higher than the threshold value, a second regime of optimal compression is realized, in which the durations of input and output pulse are influenced only by the geometrical parameters of line cross-section due to quasi-TEM dispersion processes. Due to the similarity in quasi-TEM type of dispersion, the existence of two regimes should hold true for traditional coaxial MCLs as well. Applying this distinction to the main body of experimental data on MCLs [10], [11], [12], [13], [14], it seems that in works [9], [12] mainly the first, low-voltage gyromagnetic regime of compression is realized, while in works [10], [11], [13], [14] the high-voltage quasi-TEM dispersion regime of compression is realized.

Conclusion

In this paper, a numerical analysis of parallel-plate magnetic compression line was conducted. The results of numerical experiments show that the modes of pulse shaping in such a line are analogous to those of traditional coaxial magnetic compression lines, and that traditional pulse compression mode with twofold peak power increase can be achieved, as well as single-soliton shaping and high-power microwave generation. It was also shown that at voltages over ~1 MV due to partial filling of the line with ferrite the duration of the output pulse is set by the dispersion properties of the dominant dispersive quasi-TEM wave, which is seen as the independence of output pulse duration on pulse amplitude, and its dependence on ferrite filling factor. It was found that, analogously to coaxial magnetic compression lines, the duration of output pulse in this regime is close to the roundtrip time of electromagnetic wave between line conductors. The found analogy between the processes in magnetic compression lines of parallel-plate and coaxial geometries can be used to facilitate analytical treatment of nonlinear pulse compression in such systems due to reduced complexity of the mathematical problem in parallel-plate geometry compared to coaxial one. Parallel-plate geometry might also be advantageous in practice compared to coaxial one due to the simplified fabrication process, however, for such comparison breakdown processes need to be carefully considered.

Благодарности

Автор выражает благодарность Институту физики металлов УРО РАН за возможность использования программного обеспечения COMSOL Multiphysics для проведения численного моделирования.

Конфликт интересов

Не указан.

Рецензия

Все статьи проходят рецензирование. Но рецензент или автор статьи предпочли не публиковать рецензию к этой статье в открытом доступе. Рецензия может быть предоставлена компетентным органам по запросу.

Acknowledgement

The author is grateful to the Institute of Metal Physics of UB RAS for the possibility of using COMSOL Multiphysics software to perform the numerical simulations.

Conflict of Interest

None declared.

Review

All articles are peer-reviewed. But the reviewer or the author of the article chose not to publish a review of this article in the public domain. The review can be provided to the competent authorities upon request.

Список литературы / References

1. Mankowski J. High voltage subnanosecond breakdown. / J. Mankowski, J. Dickens, M. Kristiansen // IEEE Transactions on Plasma Science. — 1998. — 3. — P. 874–881. — DOI: 10.1109/27.700858

2. Mesyats G.A. Generation of Powerful Subnanosecond Pulses (Review). / G.A. Mesyats, V.G. Shpak // Instruments and Experimental Techniques. — 1978. — 6. — P. 1457.

3. Mesyats G.A. High-power picosecond electronics. / G.A. Mesyats, M.I. Yalandin // Physics-Uspekhi. — 2005. — 3. — P. 211. — DOI: 10.1070/PU2005v048n03ABEH002113

4. Mesyats G.A. Picosecond runaway electron beams in air. / G.A. Mesyats, M.I. Yalandin, A.G. Reutova // Plasma Physics Reports. — 2012. — 1. — P. 29–45. — DOI: 10.1134/S1063780X11110055

5. Mesyats G.A. Formation of 1.4 MeV runaway electron flows in air using a solid-state generator with 10 MV/ns voltage rise rate. / G.A. Mesyats, M.S. Pedos, S.N. Rukin // Applied Physics Letters. — 2018. — 16. — P. 163501. — DOI: 10.1063/1.5025751

6. Lobanov L.N. Formation of directed wide-aperture flows of runaway electrons in air-filled magnetized diodes. / L.N. Lobanov, K.A. Sharypov, V.G. Shpak // Review of Scientific Instruments. — 2024. — 9. — P. 093301. — DOI: 10.1063/5.0218882

7. Zheltov K.A. Picosecond High-Current Electron Accelerator. / K.A. Zheltov, S.A. Korobkov, A.N. Petrenko // Instruments and Experimental Techniques. — 1990. — 1. — P. 17.

8. Elyash S.L. Detection of Electron Radiation Pulses Generated by a Subnanosecond Accelerator. / S.L. Elyash, T.V. Loiko, A.L. Yuriev // Instruments and Experimental Techniques. — 2019. — 4. — P. 528–531. — DOI: 10.1134/S002044121903014X

9. Ulmaskulov M.R. Energy compression of nanosecond high-voltage pulses based on two-stage hybrid scheme. / M.R. Ulmaskulov, G.A. Mesyats, A.G. Sadykova // Review of Scientific Instruments. — 2017. — 4. — P. 045106. — DOI: 10.1063/1.4979641

10. Gusev A.I. Solid-state repetitive generator with a gyromagnetic nonlinear transmission line operating as a peak power amplifier. / A.I. Gusev, M.S. Pedos, S.N. Rukin // Review of scientific instruments. — 2017. — 7. — P. 074703. — DOI: 10.1063/1.4993732

11. Gusev A.I. A 30 GW subnanosecond solid-state pulsed power system based on generator with semiconductor opening switch and gyromagnetic nonlinear transmission lines. / A.I. Gusev, M.S. Pedos, A.V. Ponomarev // Review of Scientific Instruments. — 2018. — 9. — P. 094703. — DOI: 10.1063/1.5048111

12. Ulmaskulov M.R. Multistage converter of high-voltage subnanosecond pulses based on nonlinear transmission lines. / M.R. Ulmaskulov, S.A. Shunailov, K.A. Sharypov // Journal of Applied Physics. — 2019. — 8. — P. 084504. — DOI: 10.1063/1.5110438

13. Alichkin E.A. Picosecond solid-state generator with a peak power of 50 GW. / E.A. Alichkin, M.S. Pedos, A.V. Ponomarev // Review of Scientific Instruments. — 2020. — 10. — P. 104705. — DOI: 10.1063/5.0017980

14. Patrakov V.E. A 100 GW, 100 ps solid-state pulsed power system based on semiconductor opening switch generator and magnetic compression lines. / V.E. Patrakov, M.S. Pedos, A.V. Ponomarev // Review of Scientific Instruments. — 2024. — 8. — P. 084709. — DOI: 10.1063/5.0209990

15. Gusev A.I. A 6 GW nanosecond solid-state generator based on semiconductor opening switch. / A.I. Gusev, M.S. Pedos, S.N. Rukin // Review of Scientific Instruments. — 2015. — 11. — P. 114706. — DOI: 10.1063/1.4936295

16. Romanchenko I.V. High power microwave beam steering based on gyromagnetic nonlinear transmission lines. / I.V. Romanchenko, V.V. Rostov, A.V. Gunin // Journal of Applied Physics. — 2015. — 21. — P. 214907. — DOI: 10.1063/1.4922280

17. Cui Y. Operation analysis of the wideband high-power microwave sources based on the gyromagnetic nonlinear transmission lines. / Y. Cui, J. Meng, L. Huang // Review of Scientific Instruments. — 2021. — 3. — P. 034702. — DOI: 10.1063/5.0040323

18. Patrakov V.E. Inherent waveguide-like dispersion of ferrite coaxial lines / V. E. Patrakov, S. N. Rukin // 9th International Congress on Energy Fluxes and Radiation Effects (EFRE-2024). — Tomsk, 2024. — DOI: 10.13140/RG.2.2.35381.49120.

19. Припутнев П.В. Формирование мощных наносекундных высокочастотных импульсов в частично заполненных ферритом коаксиальных линиях с различными дисперсионными свойствами dis.. ...Doctor of Sciences: 1.3.5 : защищена 2024-09-10 / П.В. Припутнев. — Томск: 2024. — 175 с. — URL: https://hcei.tsc.ru/ru/obrazovanie/dissertations/priputnev.html .

20. Balanis C.A. Advanced engineering electromagnetics / C.A. Balanis. — Arizona: John Wiley & Sons Inc, 2012. — 1024 p.

21. Kuester E.F. Theory of waveguides and transmission lines / E.F. Kuester. — Boca Raton: CRC Press, 2021. — 610 p.

22. Patrakov V.E. Computer simulation of multi-gigawatt magnetic compression lines / V. E. Patrakov, S. N. Rukin // Proceedings of 8th International Congress on Energy Fluxes and Radiation Effects (EFRE-2022). — Tomsk, 2022. — P. 606-611. — DOI: 10.56761/EFRE2022.S6-P-017001.

23. Patrakov V.E. Numerical simulation of picosecond magnetic compression lines. / V.E. Patrakov // International Research Journal. — 2024. — 5(143)S. — P. 1–9. — DOI: 10.60797/IRJ.2024.143.177

24. Brown W.F. Micromagnetics / W.F. Brown. — New York: John Wiley & Sons, 1963. — 143 p.

25. Ricketts D.S. Electrical solitons: theory, design, and applications / D.S. Ricketts, D. Ham. — Boca Raton: CRC Press, 2011. — 264 p.

26. Ostrovskii L.A. Solitary electromagnetic waves in nonlinear lines. / L.A. Ostrovskii, V.V. Papko, E.N. Pelinovskii // Radiophysics and Quantum Electronics. — 1972. — 4. — P. 438–446.

27. Case M. Picosecond duration, large amplitude impulse generation using electrical soliton effects. / M. Case, E. Carman, R. Yu // Applied Physics Letters. — 1992. — 24. — P. 3019–3021. — DOI: 10.1063/1.106795

Список литературы на английском языке / References in English

1. Mankowski J. High voltage subnanosecond breakdown. / J. Mankowski, J. Dickens, M. Kristiansen // IEEE Transactions on Plasma Science. — 1998. — 3. — P. 874–881. — DOI: 10.1109/27.700858

2. Mesyats G.A. Generation of Powerful Subnanosecond Pulses (Review). / G.A. Mesyats, V.G. Shpak // Instruments and Experimental Techniques. — 1978. — 6. — P. 1457.

3. Mesyats G.A. High-power picosecond electronics. / G.A. Mesyats, M.I. Yalandin // Physics-Uspekhi. — 2005. — 3. — P. 211. — DOI: 10.1070/PU2005v048n03ABEH002113

4. Mesyats G.A. Picosecond runaway electron beams in air. / G.A. Mesyats, M.I. Yalandin, A.G. Reutova // Plasma Physics Reports. — 2012. — 1. — P. 29–45. — DOI: 10.1134/S1063780X11110055

5. Mesyats G.A. Formation of 1.4 MeV runaway electron flows in air using a solid-state generator with 10 MV/ns voltage rise rate. / G.A. Mesyats, M.S. Pedos, S.N. Rukin // Applied Physics Letters. — 2018. — 16. — P. 163501. — DOI: 10.1063/1.5025751

6. Lobanov L.N. Formation of directed wide-aperture flows of runaway electrons in air-filled magnetized diodes. / L.N. Lobanov, K.A. Sharypov, V.G. Shpak // Review of Scientific Instruments. — 2024. — 9. — P. 093301. — DOI: 10.1063/5.0218882

7. Zheltov K.A. Picosecond High-Current Electron Accelerator. / K.A. Zheltov, S.A. Korobkov, A.N. Petrenko // Instruments and Experimental Techniques. — 1990. — 1. — P. 17.

8. Elyash S.L. Detection of Electron Radiation Pulses Generated by a Subnanosecond Accelerator. / S.L. Elyash, T.V. Loiko, A.L. Yuriev // Instruments and Experimental Techniques. — 2019. — 4. — P. 528–531. — DOI: 10.1134/S002044121903014X

9. Ulmaskulov M.R. Energy compression of nanosecond high-voltage pulses based on two-stage hybrid scheme. / M.R. Ulmaskulov, G.A. Mesyats, A.G. Sadykova // Review of Scientific Instruments. — 2017. — 4. — P. 045106. — DOI: 10.1063/1.4979641

10. Gusev A.I. Solid-state repetitive generator with a gyromagnetic nonlinear transmission line operating as a peak power amplifier. / A.I. Gusev, M.S. Pedos, S.N. Rukin // Review of scientific instruments. — 2017. — 7. — P. 074703. — DOI: 10.1063/1.4993732

11. Gusev A.I. A 30 GW subnanosecond solid-state pulsed power system based on generator with semiconductor opening switch and gyromagnetic nonlinear transmission lines. / A.I. Gusev, M.S. Pedos, A.V. Ponomarev // Review of Scientific Instruments. — 2018. — 9. — P. 094703. — DOI: 10.1063/1.5048111

12. Ulmaskulov M.R. Multistage converter of high-voltage subnanosecond pulses based on nonlinear transmission lines. / M.R. Ulmaskulov, S.A. Shunailov, K.A. Sharypov // Journal of Applied Physics. — 2019. — 8. — P. 084504. — DOI: 10.1063/1.5110438

13. Alichkin E.A. Picosecond solid-state generator with a peak power of 50 GW. / E.A. Alichkin, M.S. Pedos, A.V. Ponomarev // Review of Scientific Instruments. — 2020. — 10. — P. 104705. — DOI: 10.1063/5.0017980

14. Patrakov V.E. A 100 GW, 100 ps solid-state pulsed power system based on semiconductor opening switch generator and magnetic compression lines. / V.E. Patrakov, M.S. Pedos, A.V. Ponomarev // Review of Scientific Instruments. — 2024. — 8. — P. 084709. — DOI: 10.1063/5.0209990

15. Gusev A.I. A 6 GW nanosecond solid-state generator based on semiconductor opening switch. / A.I. Gusev, M.S. Pedos, S.N. Rukin // Review of Scientific Instruments. — 2015. — 11. — P. 114706. — DOI: 10.1063/1.4936295

16. Romanchenko I.V. High power microwave beam steering based on gyromagnetic nonlinear transmission lines. / I.V. Romanchenko, V.V. Rostov, A.V. Gunin // Journal of Applied Physics. — 2015. — 21. — P. 214907. — DOI: 10.1063/1.4922280

17. Cui Y. Operation analysis of the wideband high-power microwave sources based on the gyromagnetic nonlinear transmission lines. / Y. Cui, J. Meng, L. Huang // Review of Scientific Instruments. — 2021. — 3. — P. 034702. — DOI: 10.1063/5.0040323

18. Patrakov V.E. Inherent waveguide-like dispersion of ferrite coaxial lines / V. E. Patrakov, S. N. Rukin // 9th International Congress on Energy Fluxes and Radiation Effects (EFRE-2024). — Tomsk, 2024. — DOI: 10.13140/RG.2.2.35381.49120.

19. Priputnev P.V. Formirovanie moshhny'x nanosekundny'x vy'sokochastotny'x impul'sov v chastichno zapolnenny'x ferritom koaksial'ny'x liniyax s razlichny'mi dispersionny'mi svojstvami [Formation of powerful nanosecond high-frequency pulses in partially ferrite-filled coaxial lines with various dispersion properties] dis.....of PhD in : 1.3.5 : defense of the thesis 2024-09-10 / П.В. Припутнев. — Tomsk: 2024. — 175 p. — URL: https://hcei.tsc.ru/ru/obrazovanie/dissertations/priputnev.html . [in Russian]

20. Balanis C.A. Advanced engineering electromagnetics / C.A. Balanis. — Arizona: John Wiley & Sons Inc, 2012. — 1024 p.

21. Kuester E.F. Theory of waveguides and transmission lines / E.F. Kuester. — Boca Raton: CRC Press, 2021. — 610 p.

22. Patrakov V.E. Computer simulation of multi-gigawatt magnetic compression lines / V. E. Patrakov, S. N. Rukin // Proceedings of 8th International Congress on Energy Fluxes and Radiation Effects (EFRE-2022). — Tomsk, 2022. — P. 606-611. — DOI: 10.56761/EFRE2022.S6-P-017001.

23. Patrakov V.E. Numerical simulation of picosecond magnetic compression lines. / V.E. Patrakov // International Research Journal. — 2024. — 5(143)S. — P. 1–9. — DOI: 10.60797/IRJ.2024.143.177

24. Brown W.F. Micromagnetics / W.F. Brown. — New York: John Wiley & Sons, 1963. — 143 p.

25. Ricketts D.S. Electrical solitons: theory, design, and applications / D.S. Ricketts, D. Ham. — Boca Raton: CRC Press, 2011. — 264 p.

26. Ostrovskii L.A. Solitary electromagnetic waves in nonlinear lines. / L.A. Ostrovskii, V.V. Papko, E.N. Pelinovskii // Radiophysics and Quantum Electronics. — 1972. — 4. — P. 438–446.

27. Case M. Picosecond duration, large amplitude impulse generation using electrical soliton effects. / M. Case, E. Carman, R. Yu // Applied Physics Letters. — 1992. — 24. — P. 3019–3021. — DOI: 10.1063/1.106795